Paper submitted to the ASME/AIChE/ANS National Heat Transfer Conference, Session on Fundamentals of Severe Accident Analysis, Philadelphia, PA, August 6-10, 1989.

CONF-890819--22

DE89 017688

MODELING OF THERMAL AND HYDRODYNAMIC ASPECTS OF MOLTEN JET/WATER INTERACTIONS*

by

S. K. Wang, C. A. Blomquist, and B. W. Spencer

Reactor Analysis and Safety Division
Argonne National Laboratory
9700 S. Cass Ave.
Argonne, IL 60439

*Work sponsored by U. S. Nuclear Regulatory Commission.

MODELING OF THERMAL AND HYDRODYNAMIC ASPECTS OF
MOLTEN JET/WATER INTERACTIONS

by

S. K. Wang, C. A. Blomquist, and B. W. Spencer

ABSTRACT

In order to predict the effect of a fuel-coolant interaction after a hypothetical core-melt-down accident, a phenomenological model has been developed to describe the thermal and hydrodynamic behavior of a high-temperature molten jet when it interacts with saturated or subcooled water in a film boiling regime. The mechanisms of jet-material erosion were analyzed by Kelvin-Helmholtz instabilities on the coherent column and by boundary layer stripping on the leading edge. The heat transfer coefficient, vapor-film thickness, and net steam generation, all of which strongly affect the jet-breakup behavior, were solved analytically. It was found that the jet breakup (or erosion) depends strongly on the steam generation from the jet/water interaction. The jet-breakup length (i.e., penetration distance) was found to be sensitive to the initial jet temperature, water subcooling, and the physical state of the ambient water. The jet-breakup length and leading-edge velocity of the Wood's metal/water experiments are predicted well by the current model for the cases where a continuous vapor film exists.

NOMENCLATURE

C_D	= drag coefficient
C_m	= constant
d_p	= particle diameter
g	= gravitational constant
h'_{fg}	= latent heat of vaporization
Ja	= Jacob number
k	= wave number
k	= thermal conductivity
K_p	= drag constant
L/D	= breakup length in terms of jet diameter
P	= pressure
q''_R	= radiation heat flux

R = radius

r = radial coordinate

t = time

T = temperature

U = velocity

U_E = erosion velocity

V = volume

V_E = erosion volume

y = lateral coordinate

z = axial coordinate

Greek

$\langle\alpha\rangle$ = average void fraction

β = thermal expansion coefficient

δ = vapor film thickness

δ_ℓ = liquid momentum boundary layer

δ_T = liquid thermal boundary layer

ρ = density

σ = surface tension

τ = shear stress

ν = kinematic viscosity

μ = dynamic viscosity

Subscripts

ℓ = liquid (water)

v = vapor (steam)

m = melt (jet)

J = jet

L = leading edge

o = initial value

B = bubble

p = particle

s = steam

c = corium

i = interface

W = wall

SUB = subcooling

INTRODUCTION

In the event of a core-melt-down accident in a nuclear reactor, molten fuel may pour into the lower plenum or the reactor cavity where it comes into contact with water. Quenching of the melt produces steam, whose generation rate and the resulting vessel pressurization depend strongly on the degree to which the melt and water become intermixed. Thus, the extent to which the molten jet interacts with water and the physical state of the molten jet when it comes into contact with the vessel structure is a major concern in a core-melt-down accident.

The jet-breakup length has been analyzed previously by many investigators. Taylor estimated the breakup length of a liquid-metal jet in water based on this earlier study of the generation of ripples by wind blowing over a viscous fluid [1,2]. Epstein et al. [3] determined analytically the breakup length of a liquid-metal jet in water for two limiting cases: very thin and very thick vapor blankets. Those analyses assume that jet breakup is the result of the growth of infinitesimally small disturbances, and a dispersion relation is obtained to describe the erosion on the jet. However, the prediction of the jet-breakup length proposed by these investigators cannot be applied to the corium (molten core material) - water interaction for two main reasons: (1) the formation and erosion of the jet leading edge, which is believed to play an important role in jet breakup, has not been successfully analyzed, and (2) the role of the vapor film and vapor-phase velocity in the film has been overlooked.

Computer codes to predict melt-water mixing and steam generation have been developed by Corradini et al. [4], Fletcher et al. [5], and Theofanous et al. [6]. Corradini et al. treated the melt stream as a series "chunks" of uniform diameter which subdivides into smaller fragments exponentially in a dimensionless time scale, employed by Pilch [7] in his study of the breakup of water droplets in high-speed air streams. Fletcher et al. and Theofanous et al. both prescribed a length scale for the dispersed particles. Vessel pressurization, predicted by these authors is in excellent agreement with experimental data; nevertheless, the information on the jet breakup and the dispersed particle-size distribution was totally missing.

The purpose of the present work has been concentrated on the development of a model which can reasonably describe the jet-breakup mechanism and the various heat-transfer aspects based on the experimental results of the simulant-material/water and corium/water tests carried out at Argonne National Laboratory.

Modeling of Pour-Stream Breakup

Based on the observation from simulant material tests [8], a conceptual configuration of the jet when it interacts with the water has been assumed as shown in Fig. 1. In high-temperature melt tests, a vapor film is always found to blanket the pour stream and the pour stream is embedded in a highly-voided two-phase mixture as shown in Fig. 1a. A vortex ball (i.e., the leading edge), followed by a coherent jet column, is usually formed immediately after the jet submerges into the water. As the vortex ball descends in water, its size varies due to material accumulated from the jet column and material shattered by the ambient fluid. A considerable amount of particles, some rather large in size, were detached from the tail of the vortex ball while the particles dispersed from the coherent column seemed to be smaller. Finally, the jet column became symmetrical (varicose) in shape and thinner and eventually jet breakup occurred.

If the erosion of the jet material is characterized by the erosion velocities $U_{E,J}$ and $U_{E,L}$ on the jet column and the leading edge, respectively, then the dynamic governing equations of the jet can be obtained by applying mass and force balance on the coherent column and the leading edge as follows:

$$2 \frac{\partial R_J}{\partial t} = -U_{E,J}; \; R_J(o) = R_o \qquad (1)$$

$$(\rho_m + \rho_\ell/2) \frac{\partial(U_L V_L)}{\partial t} = \rho_m \int_o^{R_J(t)|\text{at column/ball interface}} (U_J - U_L)\, U_J\, 2\pi r dr$$

$$+ (\rho_m - \rho_\ell) g \bar{V}_L - \rho_m U_L \frac{\partial V_{E,L}}{\partial t}$$

$$- \frac{1}{2} C_D \rho_\ell U_L^2 \pi R_L^2 \; ; \; U_L(o) = U_J \qquad (2)$$

$$\frac{\partial \bar{V}_L}{\partial t} = \int_0^{R_J(t)|\text{at column ball interface}} (U_J - U_L)\, 2\pi r dr - \frac{\partial V_{E,L}}{\partial t} \; ; \; R_L(o) = R_J(o) \tag{3}$$

The time variations of the jet diameter, the leading-edge velocity, and the leading-edge volumn can be determined from these simultaneous differential equations if the erosion velocities on the jet column and leading edge are known. It will be shown later that the erosion velocities depend strongly on the steam generated on the column and leading edge. Therefore, the jet-breakup behavior is coupled with the jet/water thermal interaction.

Erosion Velocity on the Jet Column

The Kelvin-Helmholtz instability at the vapor/liquid interface has been discussed by many authors, (e.g., see Ref. [9]). The fastest growth rate and wave number of the interfacial disturbances were determined by differentiating the dispersion equation. Then the erosion velocity of the dispersed particles at the interface due to droplets formation is approximated by the imaginary part of the velocity of the wave with the fastest growth rate. Wang et al. [10] analyzed an inviscid parallel flow of high-temperature melt and water separated by a thin sheet of steam that could occur during a molten-jet/water interaction. They concluded that the erosion velocity of the particles dispersed from the jet surface is:

$$U_E = \frac{\left[K\rho_v \rho_m (U_v - U_m)^2 - \sigma_m k (K\rho_v + \rho_m)\right]^{1/2}}{K\rho_v + \rho_m} \tag{4}$$

where $K = (1 + \cosh k\delta)/\sinh k\delta$, and the most probable wave number, k_p, is:

$$k_p \approx \frac{2\rho_v U_v^2 K^2}{3\sigma_m K - \rho_v U_v^2 \delta} \tag{5}$$

Therefore, the erosion due to Kelvin-Helmholtz instability depends on the vapor (steam) velocity in the vapor film. The erosion on the jet column is assumed to occur solely from this type of instability.

By assuming a linear temperature profile in the vapor film and a parabolic profile for both the liquid (water) velocity and the temperature in the liquid boundary layer, as shown in Fig. 2, and by applying the integral momentum and energy equations, the vapor-film thickness, δ, vapor velocity U_v, and interfacial velocity U_i can be determined by solving the following equations:

$$\int_0^\delta \frac{\partial U_v^2}{\partial z} dy - \int_0^\delta U_i \frac{\partial U_v}{\partial z} dy - \int_0^\delta g \frac{\Delta\rho}{\bar{\rho}} dy + \int_0^\delta K_p(U_p - U_v)^2 dy + \frac{\tau_i}{\bar{\rho}} + \frac{\tau_w}{\bar{\rho}} = 0 \quad (6)$$

$$\frac{\partial}{\partial z} \int_0^{\delta_\ell} U_\ell (U_\ell - U_\infty) dy_\ell = \int_0^{\delta_T} \beta_\ell (T_\ell - T_\infty) g dy_\ell - \nu_\ell \left. \frac{\partial U_\ell}{\partial y_\ell} \right|_{y_\ell = 0} \quad (7)$$

$$\left(q_R'' - k_v \frac{\partial T_v}{\partial y}\right) - \left(-k_\ell \frac{\partial T_\ell}{\partial y_\ell}\right) = \rho_v h'_{fg} \left\{\frac{\partial}{\partial z} \int_0^\delta U_v dy + \frac{U_{E,v}}{2}\right\} \quad (8)$$

Note that the average density is used for the vapor phase to account for the entrained droplets eroded from the vapor/liquid interface into the vapor film. Assumptions associated with the average vapor density, drag force induced by erosion of jet material, interfacial shear stresses, departure of steam bubbles from the vapor/liquid interface into water, liquid momentum, and thermal boundary layers, are described in Ref. [10].

The predicted vapor velocity and vapor-film thickness during a corium jet/water interaction are shown in Figs. 3 to 6 for two ambient pressures. It can be seen that the voidage of the two-phase mixture, $\langle\alpha\rangle$, as shown in Fig. 1, has a very strong effect on the vapor film thickness and vapor velocity. The bubbles in the two-phase mixture are generated from the evaporation of water by the dispersed jet material and are from the vapor film due to surface instability. In general, a highly-voided two-phase mixture reduced the hydrostatic density difference between the vapor and liquid, and therefore, reduces the vapor velocity and allows a thicker vapor film. The vapor velocity increases rapidly near the bottom of the heated surface. Then a high entrainment rate of liquid droplets, due to the high vapor velocity, produces a high drag force that offsets the increases in the vapor velocity.

Erosion Velocity on the Jet Leading Edge

In addition to the surface instability, aerodynamic stripping also accounts for the erosion on the leading edge. Taylor [12] investigated the surface-layer stripping of a large drop in a high-speed air stream. He concluded that the surface layer is removed by tangential friction and the induced velocity in the surface layer shows a profile of boundary layer type. Assume that the jet surface layer of the leading edge is constantly dragged by the enveloping fluid, i.e., steam, and departs from the main body at the tail edge due to an abrupt change in the pressure distribution, and assume a velocity profile for the surface layer as per Taylor [12]:

$$U_m = U_{mi} \exp \left[- \frac{y_m}{C_m \sqrt{x}} \right] \tag{9}$$

The velocity and temperature profiles of the vapor and liquid adjacent to the leading edge are similar to those of the jet column except z is replaced by x and g is replaced by g sin θ, as shown in Fig. 7. In addition to Eqs. (6) to (8), two more equations are needed:

$$\frac{\partial}{\partial x} \int_0^\infty U_m^2 dy_m = \nu_m \left. \frac{\partial U_m}{\partial y_m} \right|_{y_m=0} \tag{10}$$

and

$$\mu_m \left. \frac{\partial U_m}{\partial y_m} \right|_{y_m=0} = \tau_w \tag{11}$$

The erosion velocity (or the rate change of the volume) on the leading edge can be approximated by:

$$\frac{\partial V_{E,L}}{\partial t} = \int_0^{R_L} 2\pi R_L \left. U_m \right|_{\theta=\pi/2} dR_L$$

$$\simeq 2\pi U_{mi} C_m \left(\frac{\pi R_L}{2}\right)^{1/2} \left[R_L^{\cdot} - C_m \left(\frac{\pi R_L}{2}\right)^{1/2}\right] \tag{12}$$

After the erosion velocities on the column and leading edge are calculated, the jet-breakup behavior can be completely determined.

Dispersed-Particle-Size Distribution

As described before, the diameter of the particles dispersed from the jet column due to Kelvin-Helmholtz instability is approximated by the wave length of the most unstable wave, i.e., $d_p \sim 1/k_p$. However, the particles dispersed from the tail of the leading edge may show quite a different size distribution since the erosion mechanism is completely different. Presumably, the drag-induced energy is lost at the tail in the form of the kinetic energy of dispersed particles and the formation of a new surface area. Then the particle size can be estimated by solving the following equation:

$$\frac{1}{2} \rho_m \int_0^\infty 2\pi (R_L - y_m) U_m^3 \Big|_{x=\pi R_L/2} dy_m$$

$$= \frac{6\sigma_m}{d_p} \left(\frac{\partial V_{E,L}}{\partial t}\right) + \frac{1}{8} \rho_m U_{mi}^2 \left(\frac{\partial V_{E,L}}{\partial t}\right) \tag{13}$$

For a thin corium boundary layer, Equation (13) can be simplified to yield

$$d_p \simeq \frac{144\, \sigma_m}{\rho_m U_{mi}^2} \tag{14}$$

Hence, it can be shown that the dispersed particles from the leading edge are usually ~1 to ~10 times bigger than the dispersed particles from the jet column during the corium/water interaction.

Comparisons with Jet-Breakup Experiments

Previous basic research on jet breakup has primarily been with small-diameter jets on the order to 1 mm and with low-density fluids. The majority of the currently published data is for liquid jets with low temperatures injected into gaseous atmospheres. Therefore, very limited experimental data on the high-temperature jet breakup are available. Gabor et al. [8] investigated the breakup and mixture behavior of initially coherent streams of high-density molten metals flowing into water. Molten Wood's metal was the pour-stream material for the majority of the tests. Several experiments were conducted with high-temperature melts (~600 to 750 K) so that film boiling was believed to have occurred when the jets interacted with the water. The position of the leading edge as a function of time was determined from motion-picture films. The behavior of the leading-edge velocity was used to interpret the jet-breakup process. The jet-breakup length was defined by Gabor et al. as the point where the leading edge velocity becomes the settling velocity of the dispersed particles. The measured and predicted jet-breakup length and the leading-edge velocity for tests with high-temperature melts flowing into saturated water are shown in Figs. 8 to 10. In general, the jet-breakup length and the leading-edge velocity can be predicted very well by this model for cases with high-temperature melts ($T_w > 600$ K). However, for the case of $T_w = 400$ K (Fig. 10), a premature jet-breakup length was predicted because a very thin vapor film (~0.05 mm) was calculated for such a low wall superheat. Consequently, a high-erosion velocity, which results from a high vapor velocity in the thin film, was predicted and this caused the premature jet breakup. However, under such low wall superheat, a continuous vapor film is very unlikely to exist during the interaction. Therefore, this model cannot be applied to the cases with low jet temperatures ($\lesssim$600 K). The leading-edge velocity (or jet-penetration velocity, U_p) was also analyzed by Hopkins and Robertson [12] for two dimensions and the following correlation was given:

$$K = \frac{U_J - U_p}{U_p} \left(\frac{\rho_1}{\rho_2}\right)^{1/2} \qquad (15)$$

Where K was determined experimentally for different density ratios, and the subscripts 1 and 2 denote the water and the jet, respectively. In general, the jet penetration velocity predicted by Hopkins et al. is lower than the measurements. This is probably due to the two-dimensional flow geometry used by the authors.

The effects of water subcooling on the breakup of a high-temperature corium jet for two ambient pressures is shown in Figs. 11 and 12. If the void fraction of the two-phase mixture, $\langle\alpha\rangle$, can be held constant under different conditions of water subcooling, it is clear that the effect of water subcooling is to delay the jet breakup, as shown by the dashed lines in Figs. 11 and 12. This is simply due to a lower erosion velocity resulting from lower steam generation by evaporization of water at the vapor/liquid interface. However, in reality $\langle\alpha\rangle$ depends on several parameters, such as water subcooling, initial jet temperature, and ambient pressure. The bubbles in the two-phase mixture are mainly generated from vapor departure at the vapor/liquid interface due to surface instability, and from evaporation by the jet material eroded from the jet column and the leading edge. The void fraction of the two-phase mixture is estimated by averaging the total volume of generated bubbles over a volume determined by the lateral traveling distance of the ejected jet material during the interaction. If water is subcooled, bubbles may condense or even collapse during ascension to the water surface. For a thermally-controlled collapse, Hewitt and Parker [13] proposed a semi-empirical correlation for the bubble collapse in a subcooled liquid:

$$\frac{R}{R_o} = 1 - (t_s)^{1/2} \qquad (16)$$

where

$$t_s = \frac{4}{\pi} J_a^2 \frac{\alpha t}{R_o^2} \left(\frac{R_o}{R}\right)^2 \left(\frac{1.44\ K}{\Delta T_{SUB}}\right)^{1.5}$$

Equation (16) was applied to calculate the void fraction, $\langle\alpha\rangle$, in subcooled water and these results were used to estimate the jet-breakup length, as shown by the solid lines in Figs. 11 and 12. In general, saturated water allows a jet to penetrate deeper before a complete breakup occurs. If water subcooling increases, the jet-breakup length decreases as the effect of $\langle\alpha\rangle$ prevails over that of the subcooling. Once the void fraction becomes very low as the water subcooling increases, the jet-breakup length increases again.

The effect of jet temperature predicted by the present model for a corium jet is shown in Fig. 13. The jet-breakup length shows a maximum at $T_w \sim 2000$ K if the corium does not freeze below 2950 K. Also, note that the effect of $\langle\alpha\rangle$ is implicitly represented by the jet temperature. The jet-breakup length was also analyzed by Epstein and Fauske [3] based on a linear Kelvin-Helmholtz instability and no consideration of the steam velocity. The authors derived the jet-penetration distance in a thick-steam film as follows:

$$L/D = \frac{\sqrt{3}}{2} \left(1 + \frac{\rho_s}{\rho_c}\right)\left(\frac{\rho_c}{\rho_s}\right)^{1/2} \qquad (17)$$

where the subscripts s and c denote vapor (steam) and corium (jet), respectively. Equation (17) can be expressed in terms of jet-surface temperature, and over the jet temperature range of interest, this equation overpredicts the breakup length by a factor ranging from ~2 to 10 as compared to the model presented.

Conclusions

The following conclusions may be drawn from the current analysis:

1. The breakup and quenching of a high-temperature molten jet flowing through saturated or subcooled water in a film-boiling regime has been analyzed by a simple, idealized configuration for a jet/water interaction. The erosion of jet material is calculated by assuming a Kelvin-Helmholtz type interfacial instability on the coherent column and by boundary-layer stripping on the leading edge.

2. The jet breakup (or erosion) depends strongly on the steam generated from the jet/water interaction. Therefore, the hydrodynamic behavior of the jet breakup is coupled with the jet/water thermal interaction.

3. The thermal aspects of the jet/water interaction, such as the heat-transfer coefficient, the vapor-film thickness, the steam velocity, etc., are all solved for analytically. However, experimental data on the heat-transfer coefficient for a jet with high temperature are required to validate the present model.

4. The present model has been compared with the Corium/Coolant Mixing (CCM) experiments carried out at Argonne National Laboratory [14]. A large portion of the dispersed particles were predicted to be smaller than ~1 mm, which is consistent with the visual inspection of the solidified debris.

5. The jet-breakup length (penetration distance) was found to be sensitive to the initial jet temperature, water subcooling, and accordingly, the physical state of the ambient water. For a corium jet, a breakup length of ~30 was predicted. However, the physical state of the ambient water can be affected by the vessel boundary. For instance, if the vessel is not large enough, then the boil-off of water due to jet injection may produce a highly-voided environment that yields a counter-current flow. Therefore, a scaling study on the system geometry is needed.

References

1. Taylor, G. I., "The Dispersion of Jets of Metals at Low Melting Point in Water," The Scientific Papers of G. I. Taylor, Vol. III, Ed G. K. Batchor (1940).

2. Taylor, G. I., "Generation of Ripples by Wind Blowing Over a Viscous Fluid," The Scientific Papers of G. I. Taylor, Vol. III, Ed G. K. Batchor (1940).

3. Epstein, M., and Fauske, H. K., "Steam Film Instability and Mixing of Core-Melt Jets and Water," ANS Proc., 1985 National Heat Transfer Conf., Denver, CO, August 1985.

4. Corradini, M. L., and Moses, G. A., "Limits to Fuel/cooling Mixing," Nucl. Sci. & Eng., Vol. 90, pp. 19-27, 1985.

5. Fletcher, D. F., and Thyagaraja, A., "Buoyancy-Driven, Transient, Two-Dimensional Thermo-Hydrodynamics of a Melt-Water-Steam Mixture," CLM-P790, Culham Laboratory, Abingdon, Oxfordshire, 1986.

6. Theofanous, T. G., and Amarasooriya, W. H., "Premixing of Steam Explosion: A Three-fluid Model," ANS Proc. 25th National Heat Transfer Conference in Houston, TA, July 24-27, 1988.

7. Pilch, M., "Acceleration Induced Fragmentation of Liquid Drops," Ph.D. Thesis, University of Virginia (1981).

8. Gabor, J. D., Spencer, B. W., and Cassulo, J. C., Unpublished information, 1987.

9. Lenich, V. C., Physiochemical Hydrodynamics, Prentice-Hall, Englewood Cliffs, NJ, 1962.

10. Wang, S. K., Blomquist, C. A., and Spencer, B. W., "Interfacial Instability Leading to Bubble Departure During Film Boiling on Vertical Surface," to be presented at the 26th National Heat Transfer Conf., Philadelphia, PA, August 6-10, 1989.

11. Taylor, G. I., "The Shape and Acceleration of a Drop in a High Speed Air Stream," The Scientific Papers of G. I. Taylor, Vol. III, Ed. G. K. Batchelor, University Press, Cambridge, 1963.

12. Hopkins, D. F., and Robertson, J. M., "Two-Dimensional Incompressible Fluid Jet Penetration," J. Fluid Mech., Vol. 29, Part 2, pp. 273-287, 1967.

13. Hewitt, H. C., and Parker, J. D./, "Bubble Growth and Collapse in Liquid Nitrogen," Trans. ASME, J. Heat Transfer, pp. 22-26, 1968.

14. Blomquist, C. A., Wang, S. K., Spencer, B. W., and McUmber, L., "Corium Coolant Mixing Studies," to be published.

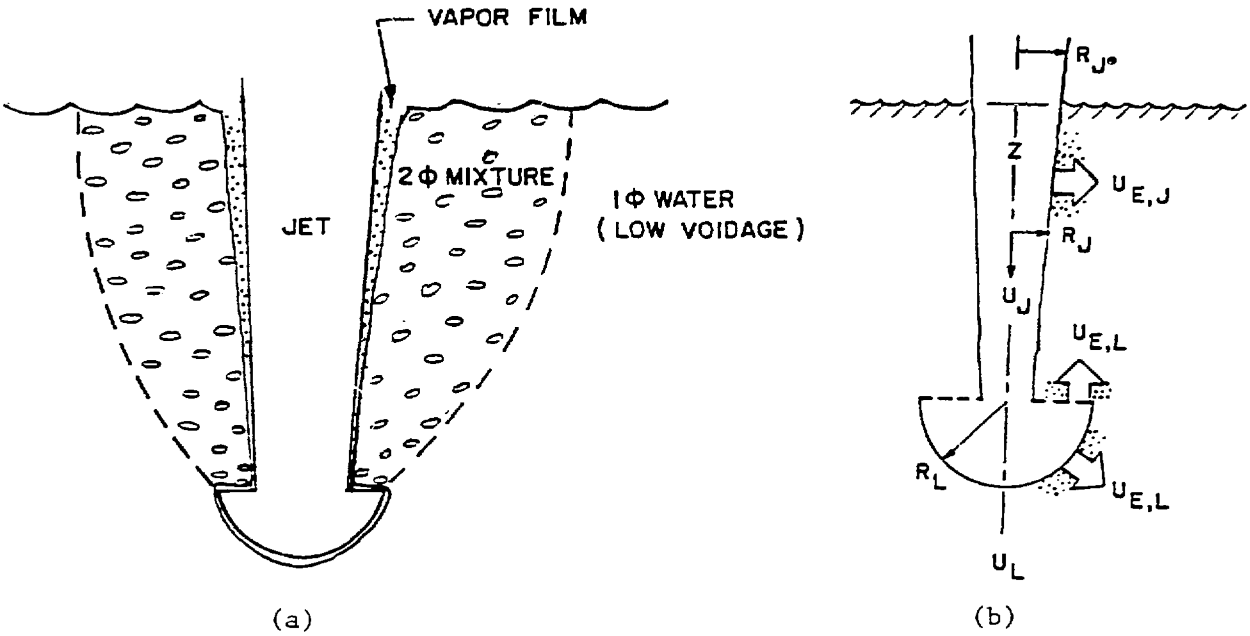

Fig. 1. Conceptual Configuration of Jet/Water Interaction

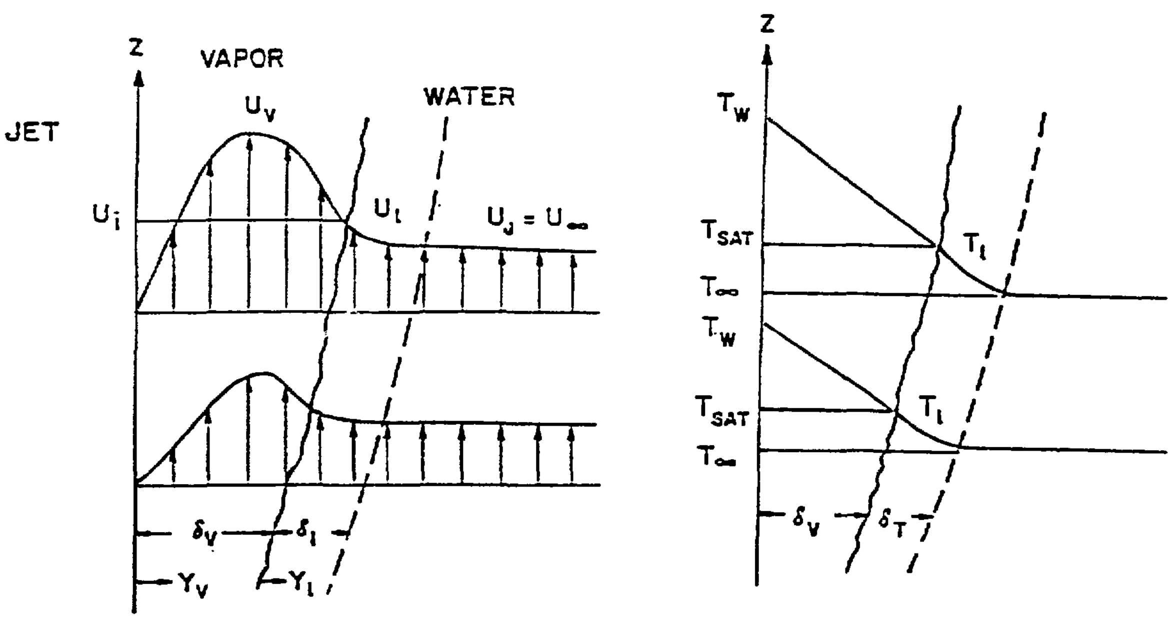

Fig. 2. Velocity and Temperature Profiles

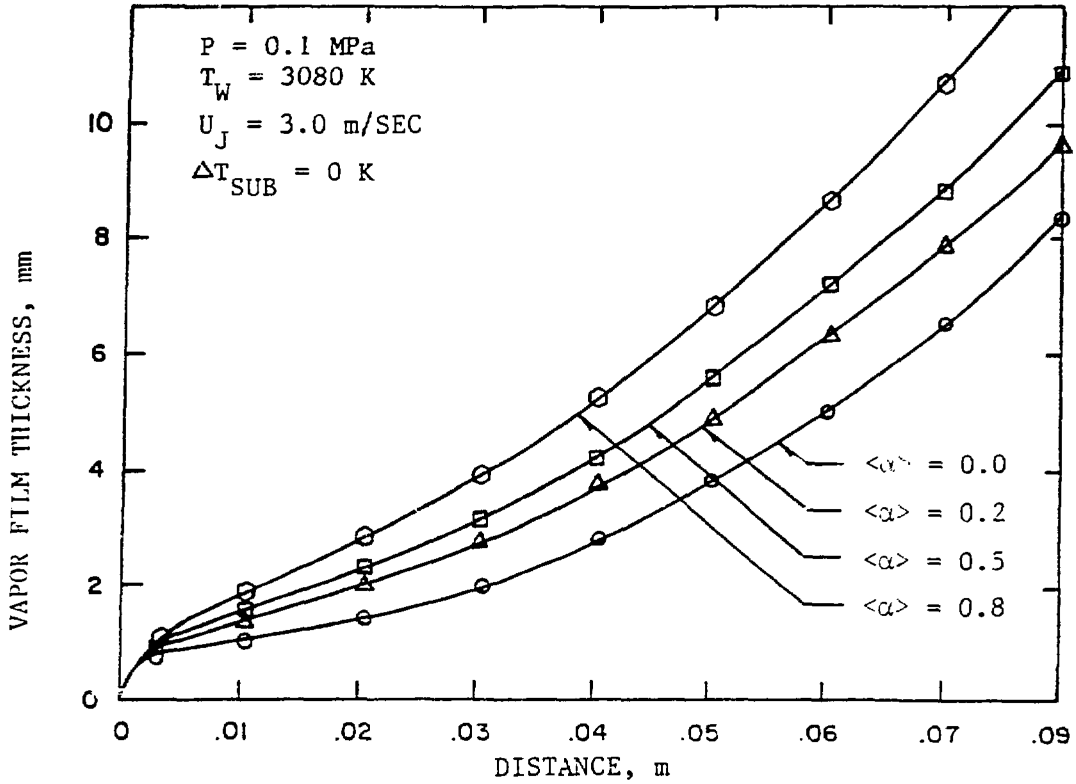

Fig. 3. Predicted Vapor Film Thickness

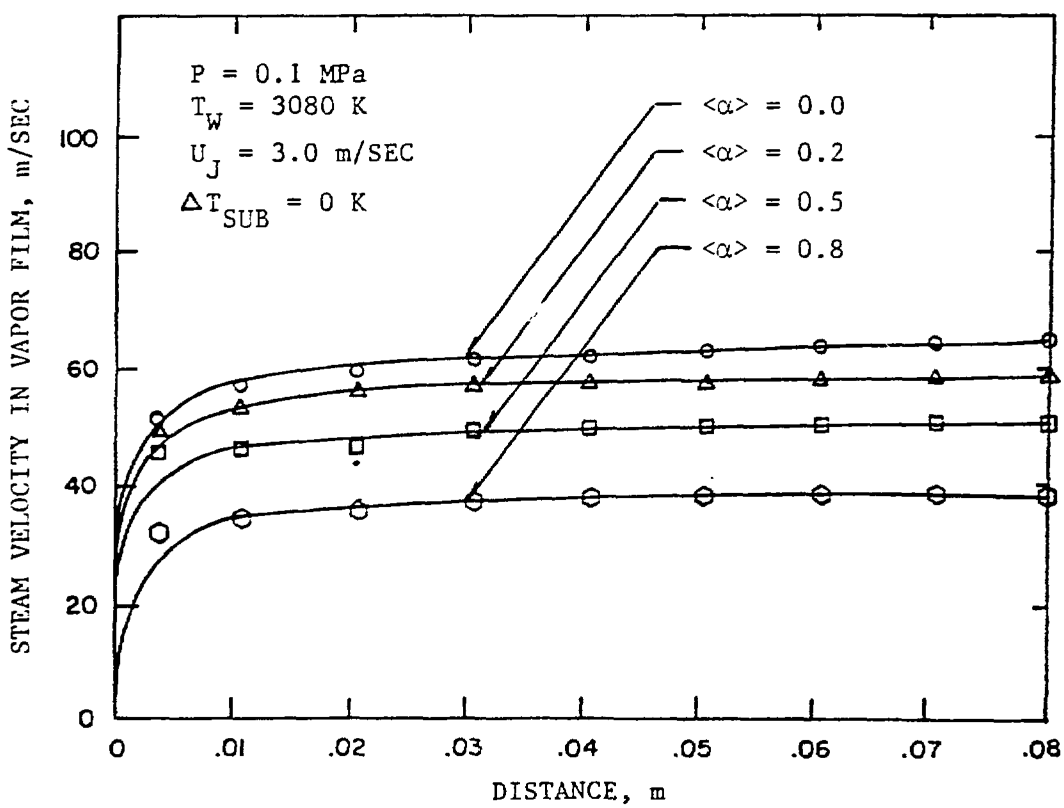

Fig. 4. Predicted Vapor Velocity

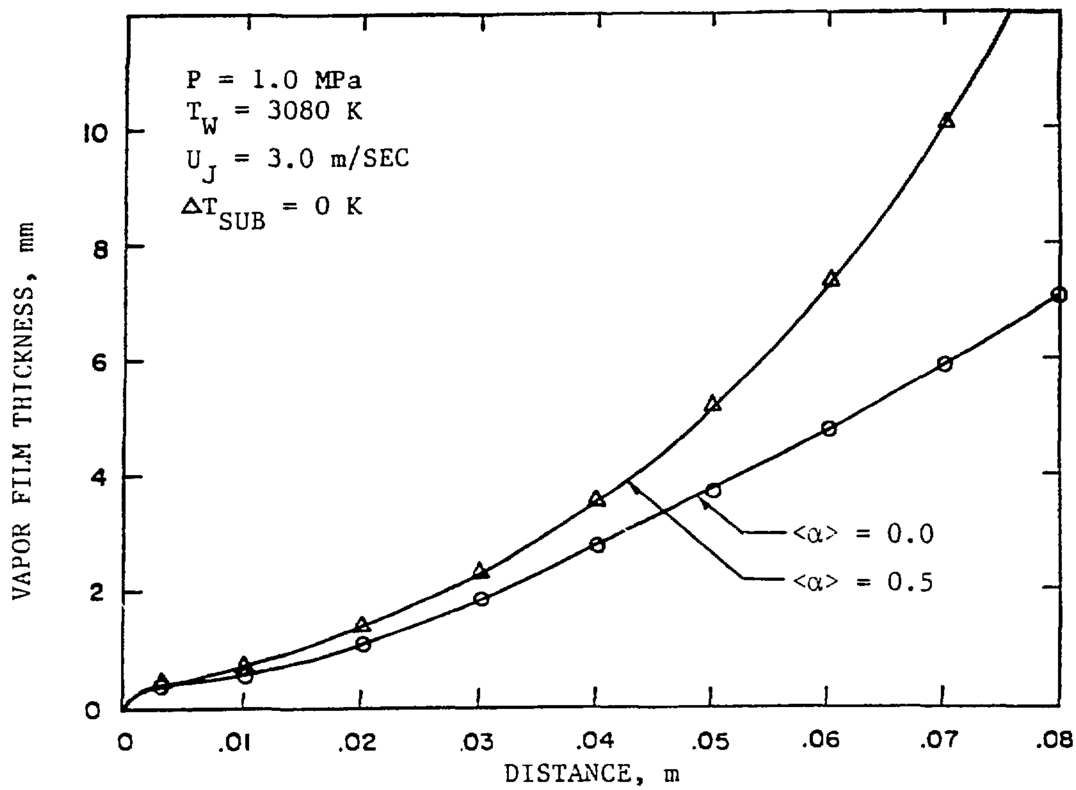

Fig. 5. Predicted Vapor Film Thickness

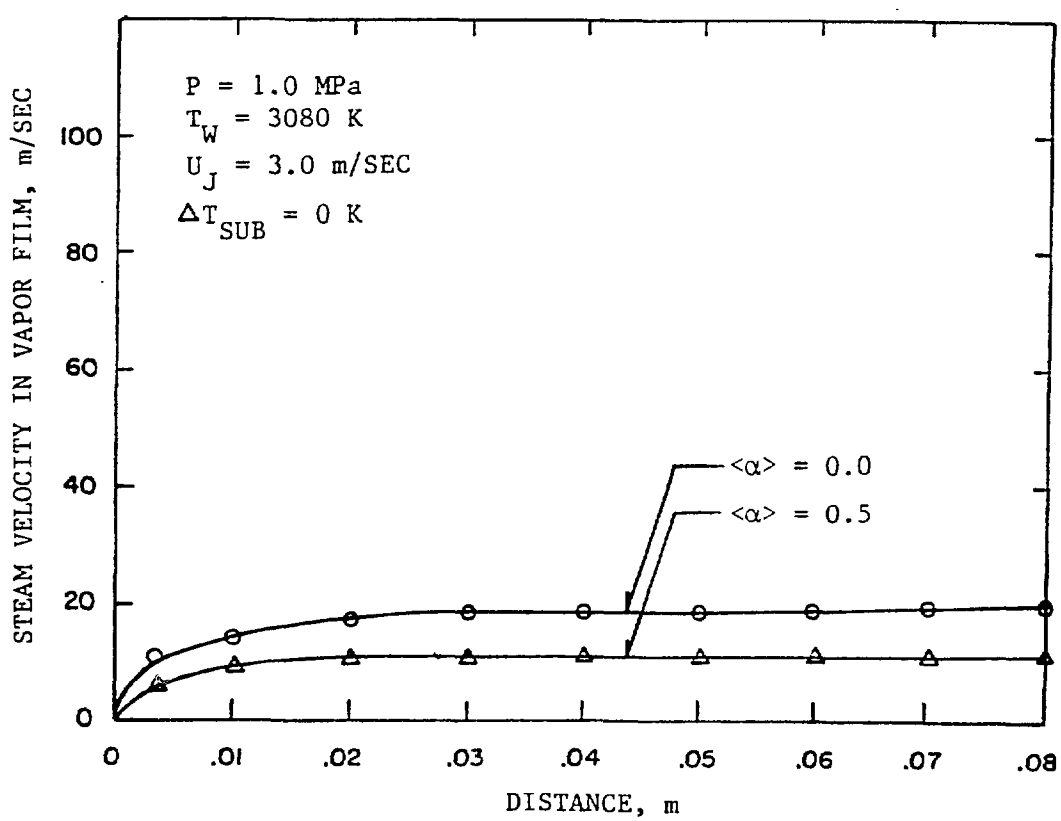

Fig. 6. Predicted Vapor Velocity

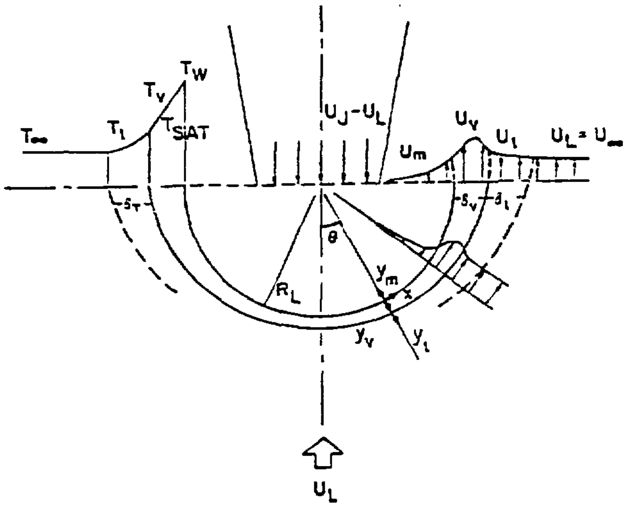

Fig. 7. Velocity and Temperature Profiles on Leading Edge

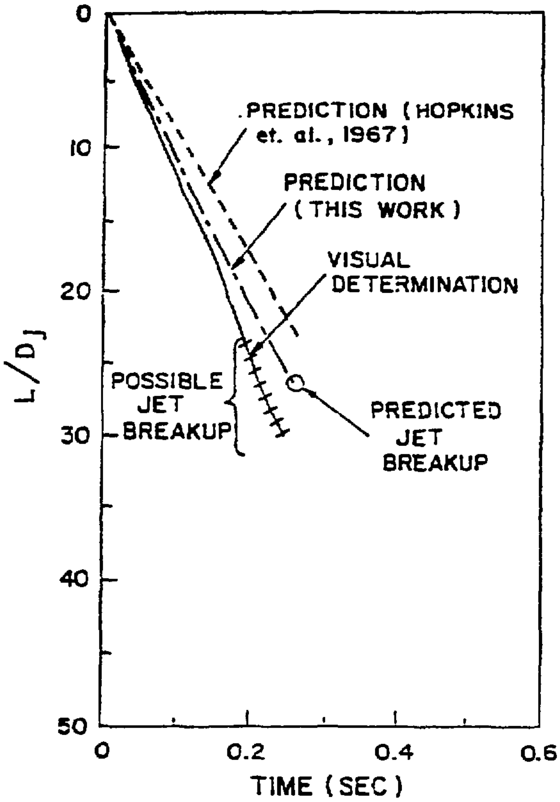

Fig. 8. Comparison of Predicted and Measured Breakup Length, JC-13, T_W=600 K

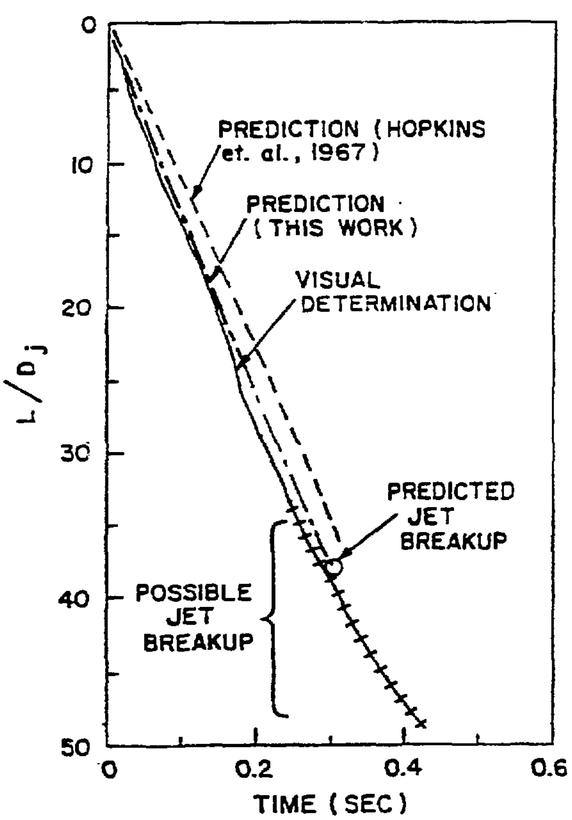

Fig. 9. Comparison of Predicted and Measured Breakup Length, JC-24, T_W=720 K

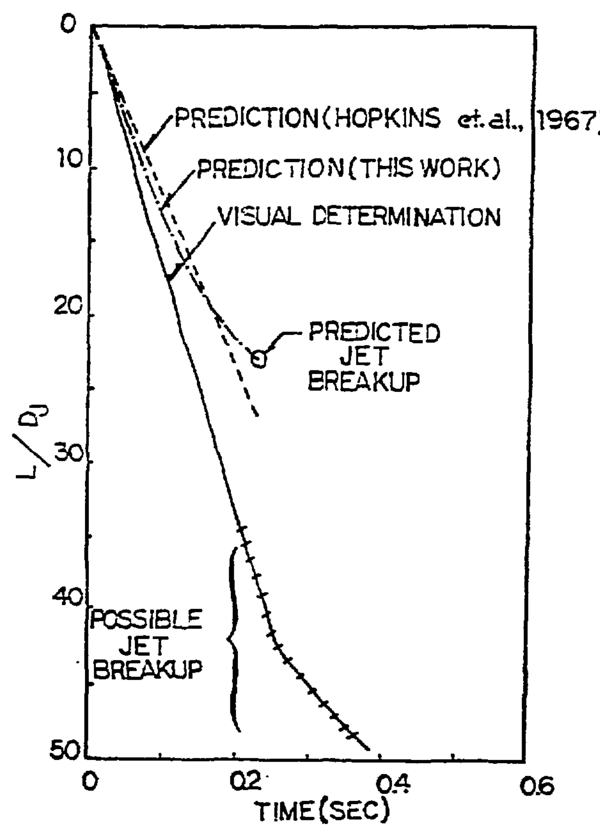

Fig. 10. Comparison of Predicted and Measured Breakup Length, JC-19, T_W=400 K

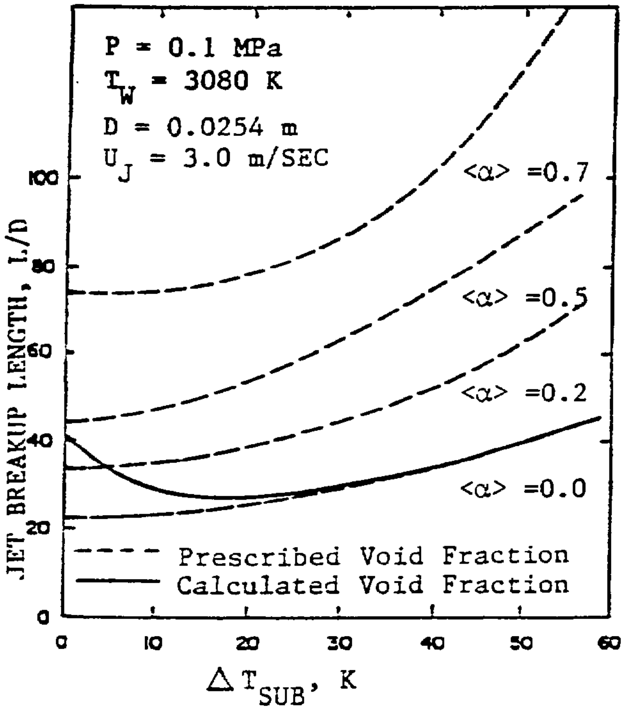

Fig. 11. Effect of Water Subcooling on Jet Breakup

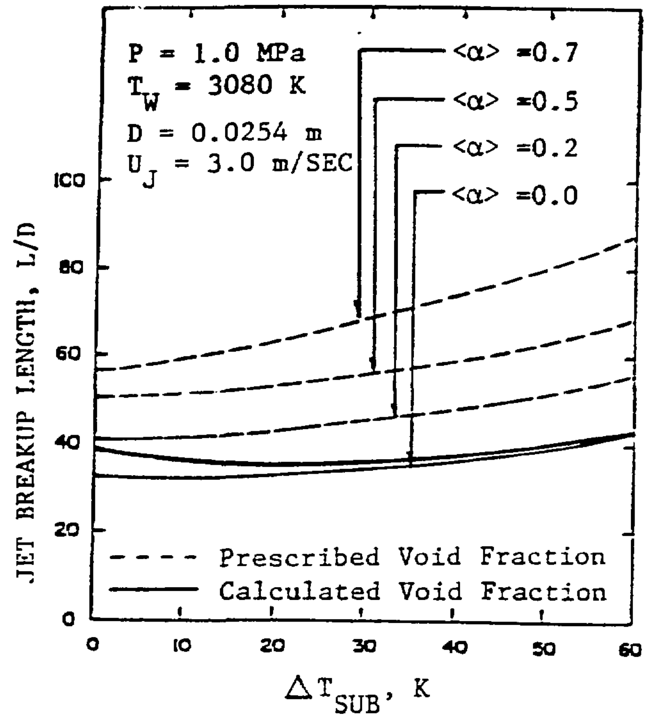

Fig. 12. Effect of Water Subcooling on Jet Breakup

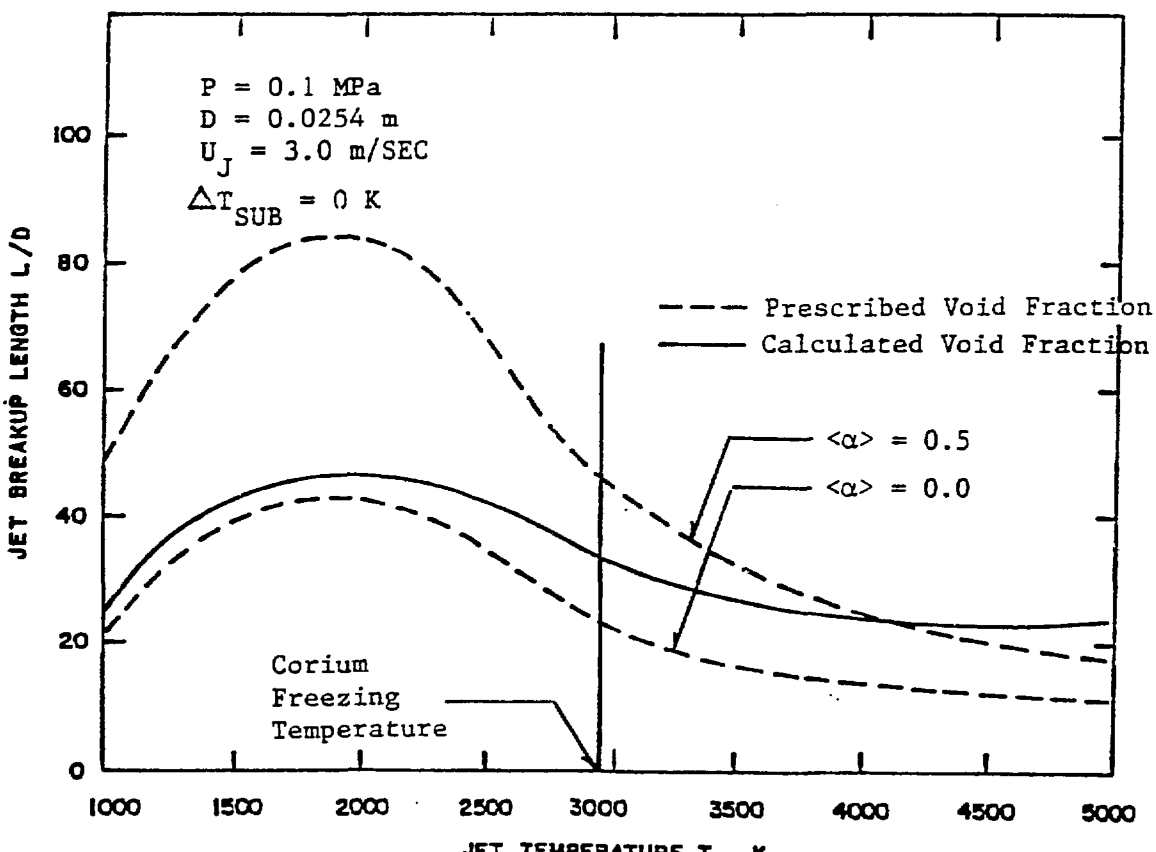

Fig. 13. Effect of Jet Temperature On Jet Breakup